

# Hot pixel contamination in the CMB correlation function

R. Aurich, S. Lustig, and F. Steiner

*Institut für Theoretische Physik, Universität Ulm,  
Albert-Einstein-Allee 11, D-89069 Ulm, Germany*

## ABSTRACT

Recently, it was suggested that the map-making procedure, which is applied to the time-ordered CMB data by the WMAP team, might be flawed by the inclusion of hot pixels. This leads to a bias in the pixels having an angular distance of  $141^\circ$  from hot pixels due to the differential measuring process of the satellite WMAP. Here, the bias is confirmed, and the temperature two-point correlation function  $C(\vartheta)$  is reevaluated by excluding the affected pixels. It is shown that the most significant effect occurs in  $C(\vartheta)$  at the largest angles near  $\vartheta = 180^\circ$ . Furthermore, the corrected correlation function  $C(\vartheta)$  is applied to the cubic topology of the Universe, and it is found that such a multi-connected universe matches the temperature correlation better than the  $\Lambda$ CDM concordance model, provided the cubic length scale is close to  $L = 4$  measured in units of the Hubble length.

**Key words:** cosmic microwave background - cosmic topology

## 1 INTRODUCTION

One of the most important observational inputs of modern cosmology is provided by the cosmic microwave background (CMB). The sky maps produced by the WMAP team (Hinshaw & et al. 2009) have found wide applications in cosmological parameter extraction and provided several surprises. Besides the low power at large scales, which had already been discovered by COBE (Hinshaw et al. 1996), some strange properties emerged concerning the statistical isotropy, i.e. an anomalous alignment between the quadrupole and the octopole (Tegmark et al. 2003; de Oliveira-Costa et al. 2004) as well as an asymmetry of the CMB fluctuations within the two hemispheres with respect to the ecliptic plane (Eriksen et al. 2004). Both anomalies are difficult to reconcile within the standard inflationary framework. A possible explanation could be related to the uncertainties which inevitably arise in the foreground removal procedure applied by the WMAP team (Gold & et al. 2009).

Recently, Liu & Li (2008a,b) have discussed a possible systematics which lies at the heart of the map-making procedure. The main point arises from the fact that WMAP measures temperature differences at two points on the sphere separated by  $141^\circ$  which is due to the construction of the probe. Hot foreground regions, which are masked later in the map-making process, do contribute in the first step in which a preliminary map is generated from the time-ordered data, i.e. the difference data. Liu & Li (2008a,b) demonstrate that the pixels, which lie on a scan ring having diameter  $141^\circ$  with a hot pixel at its centre, systematically obtain a lower temperature. They show that the corresponding

cross-correlation function displays a negative correlation at the crucial angle of  $141^\circ$  in the three frequency bands Q, V, and W thus pointing to a systematic distortion occurring in all three bands. In order to estimate the magnitude of the induced temperature distortion, Liu & Li (2008a,b) select the 2000 hottest pixels for a detailed analysis and find a temperature distortion in the range between  $11\mu\text{K}$  and  $14\mu\text{K}$  which in turn translates into a 10% difference in the quadrupole and the octopole moments. This systematics is not remedied by a prolonged observation time.

In this paper, we construct a modified mask in order to check the suggested systematics. Furthermore, the two-point temperature correlation function  $C(\vartheta)$  is investigated with respect to this systematics. With the temperature correlation function, which is based only on those pixels that are not strongly affected by this systematics, we carry out a test of a cubic topology of our Universe.

## 2 A MODIFIED LIU-LI MASK

The hot pixel systematics does not affect all pixels on the corresponding scan rings in the same way. To each hot pixel belongs a well defined scan ring, of course, but due to the large number of hot pixels there is an equally large number of affected scan rings, which intersect each other, in general. This is due to the large size of  $141^\circ$  of the scan rings. Since the systematics leads to a negative bias on a given scan ring, the bias should be more pronounced at the intersections of several affected scan rings. In order to test this effect, a modified Liu-Li mask is constructed by the following procedure.

We start with the five-year W band sky map which is

arXiv:0903.3133v1 [astro-ph.CO] 18 Mar 2009

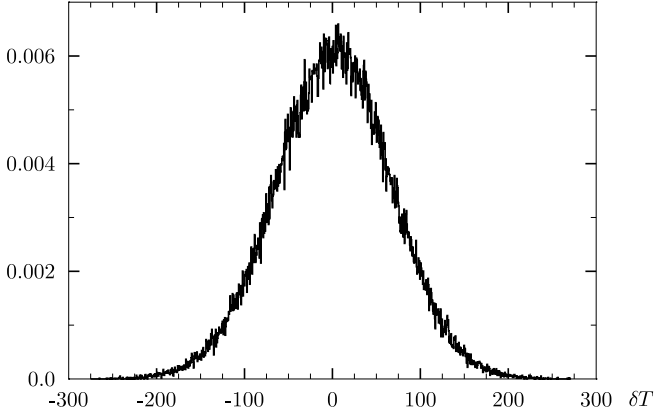


**Figure 1.** The distribution of the CMB temperature values  $\delta T$  in  $\mu\text{K}$  is shown for the ILC (5yr) map by taking into account only the pixels outside the KQ75 mask. The temperature distribution has a standard deviation of  $66\mu\text{K}$ .

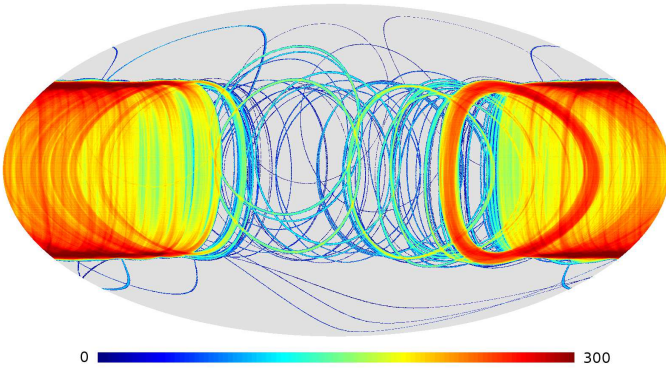


**Figure 2.** The degree of the disturbance by hot pixels is shown for the threshold  $T_{\text{thres}} = 1000 \mu\text{K}$  in Galactic coordinates. The pixels are represented in dependence on the number  $N_{\text{inter}}$  of scan rings belonging to hot pixels with  $\delta T > T_{\text{thres}}$  up to  $N_{\text{inter}} = 300$  (colour online).

not foreground reduced and thus contains the hot pixels. This map as well as the KQ75 and KQ85 masks are provided by the WMAP team (Hinshaw & et al. 2009) on the LAMBDA home page [lambda.gsfc.nasa.gov](http://lambda.gsfc.nasa.gov). Then all pixels above a given temperature threshold  $T_{\text{thres}}$  are selected as hot pixels and their corresponding  $141^\circ$  scan rings are computed. If a given pixel obtains more than  $N_{\text{inter}}$  intersections from affected scan rings, it gets masked out. This mask depends then on both thresholds  $T_{\text{thres}}$  and  $N_{\text{inter}}$ . In a last step all pixels within the KQ75 or KQ85 mask are rejected. The remaining pixels should be those being less affected by foregrounds and therefore containing the safest cosmological information.

The value of the temperature threshold  $T_{\text{thres}}$  is chosen to be many times larger than the typical temperature fluctuation of the cosmological signal. In Figure 1 the distribution of the temperature values  $\delta T$  is shown for the ILC map based on the five-year data (Hinshaw & et al. 2009) by taking into account only the pixels outside the KQ75 mask. The temperature distribution has a standard deviation of  $66\mu\text{K}$ . We choose in the following three thresholds of  $1000\mu\text{K}$ ,  $2000\mu\text{K}$ , and  $4000\mu\text{K}$ , respectively, which are very large compared to

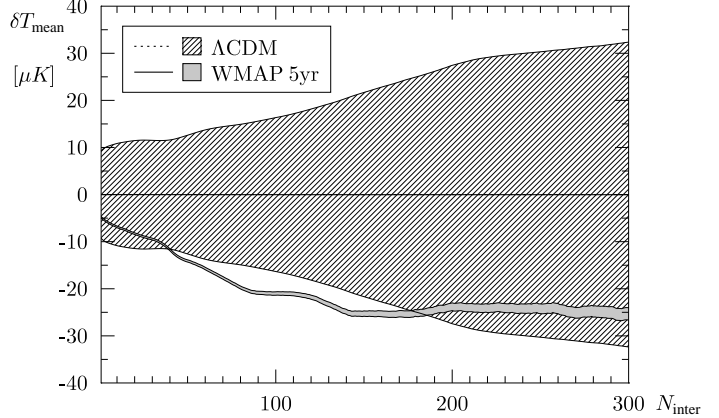


**Figure 3.** The mean temperature  $\delta T_{\text{mean}}$  is shown for the W band foreground-reduced map (5yr). The mean value is computed from the pixels inside the modified Liu-Li mask with  $T_{\text{thres}} = 1000 \mu\text{K}$  but outside the KQ75 mask in dependence on the threshold  $N_{\text{inter}}$ . The shaded region denotes the  $2\sigma$  uncertainty obtained from 100 000 simulations of  $\Lambda\text{CDM}$  models subjected to the same procedure.

the standard deviation of  $66\mu\text{K}$  of the CMB signal. In Figure 2 we show the distribution of the affected pixels for a hot pixel threshold of  $T_{\text{thres}} = 1000 \mu\text{K}$ , where the Mollweide projection is used in Galactic coordinates. The intensity of the pixels depends on the number  $N_{\text{inter}}$  of hits by scan rings of hot pixels. The scale is truncated at  $N_{\text{inter}} = 300$ . One observes that the most critical pixels lie below and above the Galactic plane opposite to the Galactic centre which is in the centre of Figure 2. This behaviour is caused by the large diameter of  $141^\circ$  of the scan rings and the fact that many hot pixels above  $T_{\text{thres}}$  are near the Galactic centre.

In order to verify the negative-temperature bias of the pixels belonging to hot pixel scan rings, the mean temperature  $\delta T_{\text{mean}}$  is computed inside the modified Liu-Li mask with  $T_{\text{thres}} = 1000 \mu\text{K}$  but outside the KQ75 mask. The mean  $\delta T_{\text{mean}}$  depends on the chosen value of the threshold number  $N_{\text{inter}}$ , i. e. pixels are selected if they are related to at least  $N_{\text{inter}}$  hot pixels. This procedure tests whether the negative bias increases with the number  $N_{\text{inter}}$  of scan rings. Figure 3 reveals that  $\delta T_{\text{mean}}$  computed for the W band foreground-reduced map indeed drops towards more negative values until a value of  $N_{\text{inter}} \simeq 140$  is reached. The pixels with  $N_{\text{inter}} \gtrsim 140$  possess a temperature bias of the order of  $-25 \mu\text{K}$ . This is the expected behaviour since with increasing  $N_{\text{inter}}$  only the most severely affected pixels are taken into account, i. e. those with the largest systematics.

In order to check the significance of this result, 100 000 simulations of  $\Lambda\text{CDM}$  concordance models are generated for which  $\delta T_{\text{mean}}$  is computed using the same procedure as outlined above. These values scatter symmetrically around a zero mean. The shaded region in Figure 3 denotes the  $2\sigma$  deviation from the zero mean. One observes that the W band distortion is over a wide range of values of  $N_{\text{inter}}$  larger than the  $2\sigma$  deviation for  $\Lambda\text{CDM}$  models. This demonstrates that there is a systematics for these pixels.

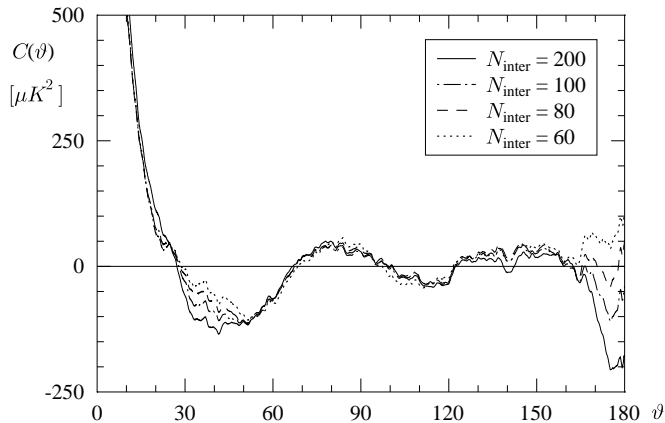


**Figure 4.** The correlation function  $C(\vartheta)$  is computed from the W band foreground-reduced map (5yr) using the pixels outside the KQ75 mask. In addition the pixels inside the modified Liu-Li mask are rejected for 4 different values of the threshold  $N_{\text{inter}}$ .

### 3 THE CORRELATION HOLE AT $\vartheta = 180^\circ$

Let us now come to the *temperature two-point correlation function*  $C(\vartheta)$ , which is defined as

$$C(\vartheta) := \langle \delta T(\hat{n}) \delta T(\hat{n}') \rangle \quad \text{with} \quad \hat{n} \cdot \hat{n}' = \cos \vartheta \quad . \quad (1)$$

It was computed by Hinshaw et al. (1996) from the COBE 4yr data and was found to display unexpectedly low power at large angles  $\vartheta \gtrsim 60^\circ$ . At these large angles  $C(\vartheta)$  is close to zero. Only near  $\vartheta = 180^\circ$  it shows a slight negative power, which is much more pronounced in the WMAP five-year data (Copi et al. 2008). This anticorrelation of antipodal points is the so-called ‘‘correlation hole’’. Copi et al. (2008) show the strong dependence of the correlation hole on the chosen mask. The correlation function  $C(\vartheta)$  possesses the largest antipodal anticorrelation by using no mask at all, whereas applying the KQ75 mask reduces the anticorrelation, but it is nevertheless present. They conclude that the full-sky results seem inconsistent with the cut-sky results. Furthermore, most of the large-angle correlation in reconstructed sky maps lies inside the part of the sky that is contaminated by the Galaxy.

In this paper we show that the remaining negative correlation near  $\vartheta = 180^\circ$  is caused by the systematic distortion introduced by hot pixels through their large scan rings as discussed above. To that aim we apply our modified Liu-Li mask with  $T_{\text{thres}} = 1000 \mu\text{K}$  together with the KQ75 mask to the W band foreground-reduced map (5yr) for several choices of the intersection threshold  $N_{\text{inter}}$ . The result shown in Figure 4 reveals a pronounced correlation hole for large values of  $N_{\text{inter}}$ , i. e. for those cases where only a small number of further pixels is rejected after applying the KQ75 mask. The curve belonging to  $N_{\text{inter}} = 200$  displays almost the usual result obtained by using only the KQ75 mask, whereas the one belonging to  $N_{\text{inter}} = 60$  gives even positive correlations near  $\vartheta = 180^\circ$ . The four cases presented in Figure 4 also demonstrate that the correlation is for other angular separations  $\vartheta$  nearly independent on the value  $N_{\text{inter}}$  except for the interval  $[30^\circ, 50^\circ]$ . However, the strongest sensitivity occurs at  $\vartheta = 180^\circ$ .

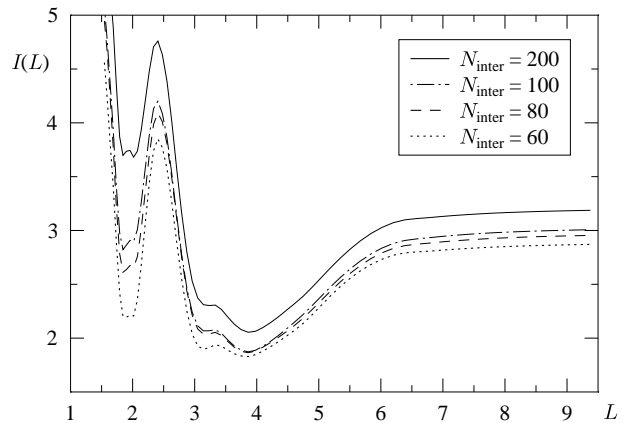


**Figure 5.** The weighted temperature correlation difference  $I(L)$  is computed from the four correlation functions  $C(\vartheta)$  shown in Figure 4. The length  $L$  denotes the size of the cubic topology measured in units of the Hubble length.

### 4 THE CUBIC TOPOLOGY FOR THE MODIFIED CORRELATION FUNCTION

The surprisingly low CMB large-angle power of the correlation function  $C(\vartheta)$ , which was discovered by Hinshaw et al. (1996), is at variance with the  $\Lambda\text{CDM}$  concordance model as has been found by Spergel & et al. (2003) and recently emphasised by Aurich et al. (2008) and Copi et al. (2008). One of the possible explanations for this unexpected behaviour is provided by models of the Universe whose spatial part is represented by a multi-connected space form. For a general introduction to the topology with respect to cosmology, see e. g. (Lachièze-Rey & Luminet 1995; Starkman 1998; Luminet & Roukema 1999; Levin 2002; Rebouças & Gomero 2004; Luminet 2008). In these models exists naturally a largest wavelength at which perturbations can occur as seeds for structure formation. This wavelength is mainly determined by the size of the topological space form. The correlation function  $C(\vartheta)$  has been studied for several multi-connected space forms, and a low large-angle power has been shown to exist in the case of the hyperbolic Picard topology (Aurich et al. 2004, 2005), the spherical Poincaré dodecahedron (Aurich et al. 2005), and the flat toroidal universe (Aurich et al. 2008).

In (Aurich et al. 2008) we have analysed the WMAP three-year data with respect to the question whether a flat toroidal universe, i. e. a cubic topology, is compatible with the CMB observations. To that aim the correlation function  $C^{\text{model}}(\vartheta)$  obtained from the cubic topology with side length  $L$  is compared to the observed correlation function  $C^{\text{obs}}(\vartheta)$  by using the integrated weighted temperature correlation difference

$$I := \int_{-1}^1 d \cos \vartheta \frac{(C^{\text{model}}(\vartheta) - C^{\text{obs}}(\vartheta))^2}{\text{Var}(C^{\text{model}}(\vartheta))} \quad . \quad (2)$$

It is found in (Aurich et al. 2008) that the results depend on the chosen mask that is applied to the CMB data. Applying the kp0 mask to the data shows that cubic topologies around  $L = 3.86$  are preferred whereas using no mask at all leads to models having a size around  $L = 4.35$ . ( $L$  is given in units of the Hubble length  $L_H = c/H_0 \simeq 4.26\text{Gpc}$  for  $h = 0.704$ .) This demonstrates the sensitivity on the pixels that

are selected for the computation of the correlation function  $C(\vartheta)$ .

Instead of using the three-year data as in (Aurich et al. 2008), we now compute the measure  $I(L)$ , eq. (2), using the updated five-year data, where we use the W band foreground reduced map. Furthermore, we apply the KQ75 mask together with the four modified Liu-Li masks discussed above. The result shown in Figure 5 is that cubic topologies slightly smaller than  $L = 4$  lead to the smallest values of  $I(L)$ , i.e. lead to the best agreement with the data. The corresponding values for the  $\Lambda$ CDM concordance model having infinite volume can also be read off from Figure 5. Since the distance to the surface of last scattering (SLS) is  $L_{\text{SLS}} = \Delta\eta L_H \simeq 14.2\text{Gpc}$  where  $\Delta\eta = \eta_0 - \eta_{\text{SLS}} = 3.329$  ( $\eta$  is the conformal time), topologies above  $L \simeq 6.6$  are so large that the SLS fits completely inside the toroidal universe. For larger models the value of  $I(L)$  saturates at the infinite limit  $L \rightarrow \infty$  corresponding to the concordance model. For all four values of  $N_{\text{inter}}$  the correlation function  $C(\vartheta)$  is in much better agreement with a cubic universe with  $L$  slightly below 4 than with the infinite  $\Lambda$ CDM concordance model. Excluding more pixels, i.e. decreasing  $N_{\text{inter}}$  from 200 to 60, produces a more pronounced second minimum around  $L \simeq 2$  which lies for  $N_{\text{inter}} = 60$  below the value of the concordance model but above the absolute minimum near  $L = 4$ . Despite this new feature, we conclude that by using the safest pixels the correlation function  $C(\vartheta)$  is best matched by a cubic cell with a size slightly smaller than  $L = 4$ .

## 5 SUMMARY

The presently best full-sky maps of the cosmic microwave background radiation are obtained by WMAP whose receivers are differential radiometers measuring the difference between two telescope beams separated by  $141^\circ$ . Liu & Li (2008a,b) discuss the possibility that the inclusion of hot pixels in the map-making process causes a bias in those pixels corresponding to a scan ring of  $141^\circ$ . Due to the large diameter of the scan rings, the affected pixels lie in a region far from the galactic plane which is usually considered to be scarcely contaminated. Here we confirm the bias found by Liu & Li (2008a,b) and, furthermore, compute the temperature two-point correlation function  $C(\vartheta)$  by taking this bias into account. The most dramatic effect of these biased pixels is the so-called correlation hole at  $\vartheta = 180^\circ$  in  $C(\vartheta)$ , which is absent by eliminating sufficiently many affected pixels. Thus, a correlation function  $C(\vartheta)$  is obtained which displays almost no correlations above all angular scales larger than  $60^\circ$ .

In Figures 1–5, we have presented our results for the modified Liu-Li mask using the threshold temperature  $T_{\text{thres}} = 1000\mu\text{K}$  and employing the KQ75 mask. We have checked that the conclusions of this paper remain the same if the KQ85 mask is used instead of the KQ75 mask and, furthermore, if the calculations are performed for the thresholds  $2000\mu\text{K}$  and  $4000\mu\text{K}$ , respectively.

Using the correlation function  $C(\vartheta)$  based on the most reliable data, a test for a universe with a cubic topology is carried out. It is found that such a model fits  $C(\vartheta)$  better than the  $\Lambda$ CDM concordance model if the side length  $L$  of

the cubic fundamental cell is slightly smaller than  $L = 4$  measured in units of the Hubble length.

## ACKNOWLEDGMENTS

HEALPix (healpix.jpl.nasa.gov) (Górski et al. 2005) and the WMAP data from the LAMBDA website (lambda.gsfc.nasa.gov) were used in this work. The computations are carried out on the Baden-Württemberg grid (bwGRiD).

## REFERENCES

- Aurich R., Janzer H. S., Lustig S., Steiner F., 2008, *Class. Quantum Grav.*, 25, 125006
- Aurich R., Lustig S., Steiner F., 2005, *Class. Quantum Grav.*, 22, 2061
- Aurich R., Lustig S., Steiner F., Then H., 2004, *Class. Quantum Grav.*, 21, 4901
- Aurich R., Lustig S., Steiner F., Then H., 2005, *Phys. Rev. Lett.*, 94, 021301
- Copi C. J., Huterer D., Schwarz D. J., Starkman G. D., 2008, arXiv:0808.3767 [astro-ph]
- de Oliveira-Costa A., Tegmark M., Zaldarriaga M., Hamilton A., 2004, *Phys. Rev. D*, 69, 063516
- Eriksen H. K., Hansen F. K., Banday A. J., Górski K. M., Lilje P. B., 2004, *Astrophys. J.*, 605, 14
- Gold B. et al., 2009, *Astrophys. J. Supp.*, 180, 265
- Górski K. M., Hivon E., Banday A. J., Wandelt B. D., Reinecke M., Bartelmann M., 2005, *Astrophys. J.*, 622, 759
- Hinshaw G., Banday A. J., Bennett C. L., Górski K. M., Kogut A., Lineweaver C. H., Smoot G. F., Wright E. L., 1996, *Astrophys. J. Lett.*, 464, L25
- Hinshaw G. et al., 2009, *Astrophys. J. Supp.*, 180, 225
- Lachièze-Rey M., Luminet J., 1995, *Physics Report*, 254, 135
- Levin J., 2002, *Physics Report*, 365, 251
- Liu H., Li T.-P., 2008a, arXiv:0806.4493 [astro-ph]
- Liu H., Li T.-P., 2008b, arXiv:0809.4160 [astro-ph]
- Luminet J.-P., 2008, in *Proceedings of the conference "Tessellations: The world a jigsaw"*, Leyden (Netherlands), March 2006 *The Shape and Topology of the Universe*
- Luminet J.-P., Roukema B. F., 1999, in *NATO ASIC Proc. 541: Theoretical and Observational Cosmology Topology of the Universe: Theory and Observation.* p. 117
- Rebouças M. J., Gomero G. I., 2004, *Braz. J. Phys.*, 34, 1358
- Spergel D. N. et al., 2003, *Astrophys. J. Supp.*, 148, 175
- Starkman G. D., 1998, *Class. Quantum Grav.*, 15, 2529
- Tegmark M., de Oliveira-Costa A., Hamilton A. J. S., 2003, *Phys. Rev. D*, 68, 123523